

Handwritten mark

NASA TECHNICAL MEMORANDUM

NASA TM-82396

POSTFLIGHT ANALYSIS OF THE SINGLE-AXIS ACOUSTIC
SYSTEM ON SPAR VI AND RECOMMENDATIONS
FOR FUTURE FLIGHTS

By R. J. Naumann, W. A. Oran,
Roy R. Whymark, and Charles Rey

January 1981



NASA

*George C. Marshall Space Flight Center
Marshall Space Flight Center, Alabama*

(NASA-TM-82396) POSTFLIGHT ANALYSIS OF THE
SINGLE-AXIS ACOUSTIC SYSTEM ON SPAR VI AND
RECOMMENDATIONS FOR FUTURE FLIGHTS (NASA)
35 p HC A03/MF A01 CSCL 20A

N81-18800

Unclas

G3/71 41497

1. REPORT NO. NASA TM-82396	2. GOVERNMENT ACCESSION NO.	3. RECIPIENT'S CATALOG NO.	
4. TITLE AND SUBTITLE Postflight Analysis of The Single-Axis Acoustic System on SPAR VI and Recommendations for Future Flights		5. REPORT DATE January 1981	6. PERFORMING ORGANIZATION CODE
7. AUTHOR(S) E. J. Naumann, W. A. Oran, Roy R. Whymark,* and Charles Rey*		8. PERFORMING ORGANIZATION REPORT #	
9. PERFORMING ORGANIZATION NAME AND ADDRESS George C. Marshall Space Flight Center Marshall Space Flight Center, Alabama 35812		10. WORK UNIT NO.	11. CONTRACT OR GRANT NO.
12. SPONSORING AGENCY NAME AND ADDRESS National Aeronautics and Space Administration Washington, D.C. 20546		13. TYPE OF REPORT & PERIOD COVERED Technical Memorandum	
15. SUPPLEMENTARY NOTES Prepared by Space Sciences Laboratory * Intersonics, Inc. employees		14. SPONSORING AGENCY CODE	
16. ABSTRACT This report presents the postflight analysis of the single-axis acoustic levitator that was flown on SPAR VI in October 1979. The apparatus malfunctioned. The results of a series of tests, analyses, and investigation of hypotheses that were undertaken to determine the probable cause of failure are presented, together with recommendations for future flights of the apparatus. The most probable causes of the SPAR VI failure were (1) lower than expected sound intensity due to mechanical degradation of the sound source and (2) an unexpected external force that caused the experiment sample to move radially and eventually be lost from the acoustic energy well.			
17. KEY WORDS		18. DISTRIBUTION STATEMENT Unclassified--Unlimited <i>R J Naumann</i>	
19. SECURITY CLASSIF. (of this report) Unclassified	20. SECURITY CLASSIF. (of this page) Unclassified	21. NO. OF PAGES 35	22. PRICE NTIS

TABLE OF CONTENTS

	Page
INTRODUCTION	1
ANALYSIS OF THE OPERATION OF THE SINGLE-AXIS ACOUSTIC SYSTEM ON SPAR VI.....	1
A. Impulsive Hypothesis.....	5
B. Continuous-Force Hypothesis.....	6
C. Instabilities Resulting from Nonisothermality.....	7
D. Misalignment of Vibrator/Reflector.....	8
CONCLUSIONS.....	8
APPENDIX I - ANALYSIS OF DAMPING.....	11
APPENDIX II - TEMPERATURE DEDUCED FROM SAMPLE POSITION.....	13
APPENDIX III - IMPULSIVE FORCE REQUIRED TO PRODUCE OBSERVED MOTION	15
APPENDIX IV - ANALYSIS OF IMPULSE FROM BUBBLE RUPTURE.....	17
APPENDIX V - EFFECT OF STEADY FORCE ON SAMPLE MOTION.....	18
APPENDIX VI - CONDITIONS FOR RESONANCE.....	19
APPENDIX VII - RADIAL AND AXIAL RESTORING FORCES.....	21
APPENDIX VIII - POSITIONING STABILITY AND CAPTURE AND ACOUSTIC WELL STRENGTH.....	24
APPENDIX IX - SUMMARY REPORT OF FATIGUE TESTS OF CYLINDRICAL VIBRATORS.....	27
APPENDIX X - SUMMARY REPORT OF GROUND-BASED TESTS ON ACOUSTIC LEVITATOR.....	29
APPENDIX XI - KC-135 TESTING OF THE ACOUSTIC LEVITATOR FURNACE SUBASSEMBLY.....	30

TECHNICAL MEMORANDUM

POSTFLIGHT ANALYSIS OF THE SINGLE-AXIS ACOUSTIC SYSTEM ON SPAR VI AND RECOMMENDATIONS FOR FUTURE FLIGHTS

INTRODUCTION

The technique of containerless processing offers definite advantages in the preparation of unique glassy metals and nonviscous oxide glasses. The single axis acoustic suspension/furnace device is one of the major containerless processing systems and is being developed by Intersonics, Incorporated, of Chicago, Illinois, for the Materials Processing in Space program. This device will have the capability of positioning specimens in a microgravity environment at temperatures up to 1600°C.

The initial test of operations of the device in a microgravity environment occurred in the fall of 1979 on the Space Processing Applications Rocket (SPAR) VI flight. During the approximately 5 min of microgravity, the device should have deployed, positioned, heated, melted, superheated, cooled, solidified, and captured a free floating glassy specimen. In fact, while it appeared the specimen was deployed and initially positioned, it moved out of the acoustic well and was melted and solidified on a wire.

This report analyzes the data available after the flight and that accumulated during the preflight tests to better understand the operation of the system during the SPAR VI flight and to make recommendations for the next test flight.

ANALYSIS OF THE OPERATION OF THE SINGLE-AXIS ACOUSTIC SYSTEM ON SPAR VI

Review of the flight films and telemetry data, inspection of the flight hardware, and detailed discussions with Intersonics, Incorporated, personnel have revealed the following situation with the SPAR Single Axis Acoustic System (SAS).

The SAS appeared to deploy, position, capture, and heat the sample. However, the sound intensity was lower than expected, and the sample drifted into the wire restraining cage approximately 37 s after deployment.

The sample was deployed and initially captured successfully. The sample oscillated initially in the axial direction with an amplitude of 0.7 cm and a period of 3.33 s, indicating a restoring force of 2.9 dyne/cm. Figure 1 presents the axial and radial motion of the specimen from analysis of the flight film by Marshall Space Flight Center (MSFC), while Figure 2 shows an analysis by Intersonics, Incorporated. After approximately 17 s, the amplitude had decayed to 0.5 cm and the period had increased to 4.38 s, indicating a restoring force of 1.6 dyne/cm. The decay in amplitude agrees with the damping expected from air drag (Appendix I). The decrease in restoring force can be explained from the temperature rise of the air in the furnace after the sample was injected (Appendix II).

The restoring force inferred from the axial motion of the sample was a factor of 5.5 lower than expected by Intersonics. The expected value was based on the measured amplitude of the vibrator in the pre-flight tests and the fact that the previous KC-135 flight tests showed a twofold higher restoring force in low g than in one-g. This twofold increase is believed to be the result of the removal of the loading from the weight of the vibrator in its support clamp, which presumably increases the Q. It was conceded, however, that this increase had been observed with cylindrical vibrators. No low-g data were available for the dumbbell configuration used on SPAR VI. Since the Q of the dumbbell configuration is considerably lower than the cylindrical configuration, presumably because of the additional atmospheric loading, it is not clear that there is reason to expect a twofold increase in performance in low g.

The measured amplitude of the vibrator decreased from the pre-flight value of 2.1 mils to 1.3 mils in the postflight test. The performance of the electronics and driver coil was verified by using a good vibrator, thereby confirming a degradation in the vibrator assembly. A second test using a new gasket produced the same result, indicating that the fault is in the metal vibrator itself. There is no way to determine when this degradation occurred. The telemetry only shows audio amplifier output, which was normal throughout the flight. Unfortunately, this does not relate to acoustic power delivered by the vibrator. If the vibrator had degraded before the flight (e.g., during the 4.5 min pre launch test), this could account for the observed lower performance.¹

There are limited data on the fatigue lifetime of the dumbbell vibrators. Intersonics has built only four such vibrators. One has operated for 16 h and another for 2 h without degradation. A third unit degraded after only 30 min, with the amplitude falling from 2.2 to 1.7 mils. This unit was driven at 15 A, which is considerably more than the other units. The flight unit had only 20 min of operating time and

1. The cooling fans were turned off before the flight because the vibration interfered with another experiment. It is conceivable that this loss of cooling allowed the vibrator to become hot enough near the face to anneal. This could explain the loss of performance observed between pre- and postflight.

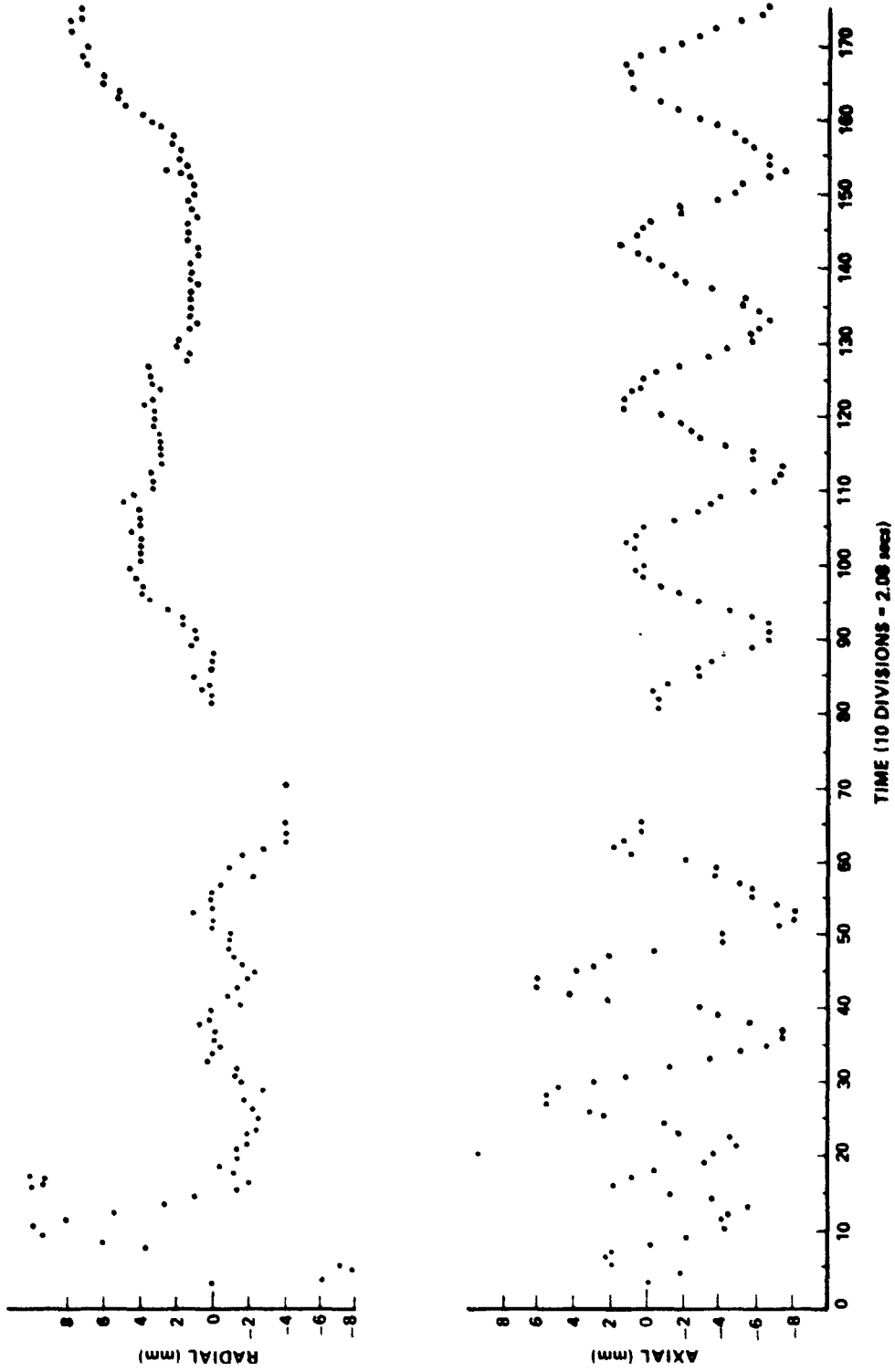


Figure 1. Measurements of the motion of the oxide specimen in the chamber. (Data were analyzed at MSFC by projecting the film image on a geometrical grid and measuring the position frame by frame. Estimated relative error of the points is ± 0.3 mm. Estimated absolute error of the radial position is ± 1 mm.)

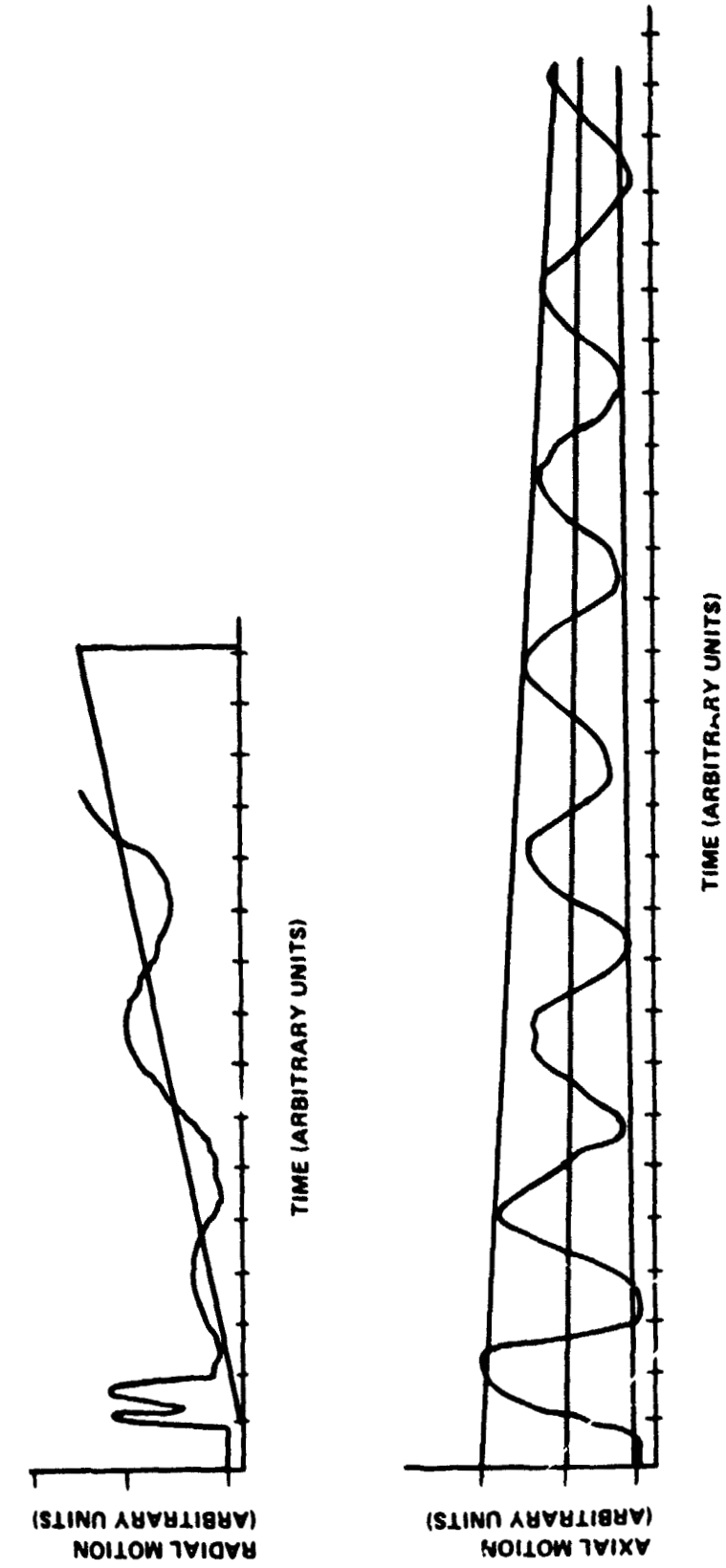


Figure 2. Measurements of the motion of the oxide specimen in the chamber as made by Intersonics, Inc. (Positional data were determined by projecting flight film on a wall and in real time approximating the position by tracing the motion.)

was driven at only 9 A. R. Whymark, of Intersonics, Incorporated, estimates the vibrator was operated at one-third of its low frequency fatigue limit and one-fifth of its ultrasonic fatigue limit based on calculations by Kuzmenko.² Inspections using dye penetrants were inconclusive. Tests by the Materials and Processes Laboratory at MSFC show that the flight vibrator does not have apparent microcracks, while a supposedly unfailed vibrator had easily observable microcracks. Whymark reports that a fatigue crack in a driver is usually extremely small and difficult to detect except by the degraded performance. Cylindrical drivers show a loss of Q and a skewed frequency distribution. The dumbbell vibrators have too low a Q when operated in air for this to be a sensitive test. Q measurements in a vacuum may reveal a detectable change but have not been done. The other failed vibrator did exhibit the characteristic skewed frequency response, but the flight vibrator did not.

Although the lower than expected acoustic performance probably contributed to the loss of the sample at approximately 37 s, this was not the primary cause. Analyses of the motion of the sample by Intersonics show an oscillation in the radial direction superimposed on a continuous drift for the sample perpendicular to the acoustic axis (Figs. 1 and 2). This is very puzzling and has not been seen previously in ground tests using a pendulum or in KC-135 flights. The oscillations indicate a restoring force of approximately 0.1 dyne/cm, which corresponds approximately to the expected radial restoring force for the acoustic field indicated by the axial oscillations. The MSFC analysis (Fig. 1) of sample motion suggests an abrupt change in radial velocity at approximately 35 s after sample deployment that carried the sample into the restraining cage. This change would correspond to an impulse of 4.4×10^{-4} g-s. The Intersonics analysis suggests this motion is a continuation of the radial oscillation superimposed on the more or less constant radial drift. The scatter in the data, resulting from the difficulty of locating the center of the sample as its temperature approaches the cavity temperature, is such that neither interpretation can be ruled out. However, a radial drift is evident in both analyses.

Several possible explanations for the observed radial motion have been suggested. Let us consider the possibilities.

A. Impulsive Hypothesis

The MSFC analysis indicated an abrupt change in radial velocity at $T + 32$ s. An impulse of 4.4×10^{-4} g-s or a steady acceleration of 1.2×10^{-4} g over the 2.3 s interval would have been required to produce this motion (Appendix III).

2. L. Kuzmenko, Fatigue Strength of Structural Materials at Sonic and Supersonic Loading Frequencies, Ultrasonics, January 1975, p. 21.

1. Vehicle Accelerations. No g spike was observed on the accelerometer corresponding to this time. The accelerometer data set an upper limit of approximately 10^{-4} g-s on the linear impulse that could have occurred during this interval. Since the Intersonics package is located approximately 1.75 m farther from the center of mass than the accelerometer package, an impulsive angular acceleration giving a tumble of 0.002 rad/s about the center of mass could account for the observed motion. This would register an impulse of only 5.5×10^{-5} g-s on the accelerometer and could have escaped detection. It was suggested that an examination of the motions of a liquid droplet in the JPL-SPAR VI experiment could show evidence of spurious angular accelerations.

Preliminary examination of Wang's flight films reveals that the sample was being oscillated by modulating the sound field during this time, making it very difficult to identify any extraneous perturbing forces.

2. Outgassing from Sample. Outgassing or a sudden ejection of gas from a bubble in the sample was considered. Since samples usually rotate perpendicularly to the acoustic axis in a single-axis levitator, it is possible to maintain a thermal gradient across the sample if the heating is asymmetric. This could lead to outgassing preferentially in one direction. It is difficult to imagine, however, how a significant temperature gradient could develop across the sample in an isothermal furnace. It was learned that the four glo-bar heaters were operated two-at-the-time, alternating every 8 s. However, the period of oscillation was considerably longer than this cycle time. Also, there was no evidence of asymmetrical heating in the image of the sample. Furthermore, the observed drift was along the direction of the glo-bars, which virtually rules out any asymmetrical heating.

3. Rupture of Bubble in Sample. The possibility of a gas bubble rupturing near the surface of the sample was considered. There is no evidence that this occurred, but it cannot be ruled out as a possibility. The bubble size required to produce the observed impulse would be several millimeters (Appendix IV). A bubble this large seems unlikely.

B. Continuous-Force Hypothesis

1. Centrifugal Force from Vehicle Rotation. The Intersonics analysis suggested the presence of a more or less continuous force superimposed on the radial restoring force, causing the sample to drift into the cage. A slow roll of the vehicle could supply a steady force that would distort the weak radial restoring force. The resulting motion associated with the combination of the two forces is discussed in Appendix V. It is concluded that the addition of a constant force would only shift the oscillation by a fixed amount. Also, the levitator is located closer to the longitudinal axis than the accelerometer package. Therefore, any vehicular motions about the longitudinal axis sufficient to cause the observed motion would have been seen on the accelerometer.

2. Resonance Hypothesis. The forces required to produce the observed radial drift would have to consist of a time-varying repulsive force that diminishes with radius superimposed on the normal restoring force. This strongly suggests some sort of resonant condition from wall reflections that strengthen with time. It is shown in Appendix VI that such a resonance condition is met as air temperature approaches 1537°C. Air temperature, as a function of time, was inferred from the analysis in Appendix II, and it is clear that the resonance condition is approached as the furnace comes back up to temperature following the injection of the relatively cold sample and related apparatus.

Without knowledge of the Q of the chamber, quantitative estimates of the strength of the high energy region near the acoustic axis are not possible. However, the qualitative features of the observed potential seem to be matched by the acoustic resonance hypothesis. The remaining question is why this effect was not observed during ground tests or in previous KC-135 flights.

One possible explanation is that the tests conducted on the ground with a pendulum did not exercise the sample injector, but instead were conducted after the system had returned to thermal equilibrium. It is also possible that the test conditions did not correspond to resonant temperatures or that the constraints involved in using the pendulum may have been such that the resonance effect went undetected.

In the early KC-135 tests, the sample was injected with the sample holder, but the sides of the furnace were opened to allow better viewing of the sample. This resulted in a decrease in furnace temperature rather than an increase and, therefore, possibly a move farther from resonance.

Several tests were recommended and carried out to establish whether or not the resonance effect was indeed the explanation for the peculiar radial drift:

1) Using the spring pendulum, the energy field was mapped as a function of temperature, including the temperatures corresponding to resonance. No measureable or visible resonance was found over the entire temperature range from 900°C to 1600°C shown in Appendix X

2) At room temperature attempts were made to induce a radial resonance in an appropriately scaled down furnace cavity. No significant resonance was observed.

C. Instabilities Resulting from Nonisothermality

Several instabilities have been observed in one-g when the sample temperature is several hundred degrees different from the ambient conditions. These instabilities have been shown to arise from the destruction of the acoustic energy well by the strong convective flows driven by the thermal gradients between the sample and the surrounding atmosphere. Whether or not these instabilities still exist in low-g because of the variations of the local sound velocity is not known.

Although there were severe temperature gradients in the furnace when the cold sample, reflector, and cage were injected into the 1600°C furnace, it would seem that instabilities arising from this effect should show up immediately, rather than after approximately 37 s, when the air temperature had almost recovered and the sample temperature had approached melting. The fact that capture and retention for the first 35 s was normal except for the drift in the radial direction makes this hypothesis seem unlikely.

Again, using the spring pendulum, a series of recommended tests were made to study the effects resulting from the sudden insertion in the furnace of cold reflectors and sample injectors. No instabilities were observed (Appendix X).

D. Misalignment of Vibrator/Reflector

The possibility of misalignment between the vibrator and reflector was considered. Since the acoustic well is established by interference between the incident and reflected waves, the energy nodes should lie along a perpendicular to the reflector. The acoustic well shifts approximately 1 cm along the axis as the temperature changes. The radial drift that could be produced by a misalignment would be $l \sin \theta$, where θ is the angle of misalignment. It is estimated that $\theta \sim 10^\circ$ would have been noticed on the film; hence the maximum radial drift that could be expected from this effect would be 0.17 cm. This cannot account for the observed 1.2 cm drift.

CONCLUSIONS

The sample was lost from the acoustic well for two reasons: lower than expected sound intensity, and an unexpected force that caused the sample to move radially.

It is known that the performance of the vibrator was substantially lower in the postflight test than in preflight. The observed loss in performance is sufficient to explain the lower sound field. Such degradation in performance is almost certainly due to a mechanical microfracture or other physical change in the metal, although this has not been verified. It is tentatively concluded that the vibrator degraded between the time it was tested in the laboratory and the time the sample was deployed during flight. It should also be recognized that the resultant force on the specimen was therefore lower than for any previously successful capture either in the laboratory or on KC-135 flights (Appendix VIII, Table 1).

There is no inherent reason why the dumbbell vibrators used in the present configuration should not work. They are limited in output and probably cannot be pushed higher than approximately 151 dB without the risk of fatigue. Indeed, fatigue analysis by MSFC of the four dumbbell vibrators produced to date by Intersonics shows distinct microcracks

in three of them; their nominal output during testing was approximately 151 dB. Some increase could probably be obtained by modifying the thermal grate to make it more transparent. This would increase the restoring force by a factor of up to 2.5. We think this is marginal to guarantee success, but if vehicle disturbances can be kept below 10^{-3} g-s, the sample should be retained in the potential well. For the next flight, we will reconfigure the SPAR package to accommodate the cylindrical vibrator. We have much more experience with this system, and it is to be used in the Materials Experiment Assembly (MEA) levitator. Also, its higher Q allows substantially higher restoring forces to be generated to insure against unanticipated low-level accelerations such as may have been encountered on SPAR VI (Appendix VII).

Also, the amplitude of the vibrator will be telemetered in addition to the amplifier output. This can be taken off the capacitive sensor on the rear of the vibrator which is fed to the input of the driver amplifier. This will permit observation of any degradation of the vibrator.

Fatigue testing of 10 cylindrical vibrators used in the St. Clair sound source has been carried out. End deflections of up to 6 mil peak-to-peak have been obtained. No failures have been observed in 5 vibrators which have been cycled at 5 mil peak-to-peak for periods of more than 4 hours with no failures. One apparent failure resulting in a slight degradation of output amplitude occurred after 10,000,000 cycles at an amplitude of 6.3 mils peak-to-peak (Appendix X).

We concluded that vibrator amplitudes up to at least 4 mils peak-to-peak can be obtained indefinitely.

A discrepancy may exist in the time required to melt the sample. Expected melting time, based on Dr. Happe's experiments was approximately 20 s. According to an evaluation of the flight film by Dr. Happe, the sample was apparently not molten at 20 s. At 37 s the sample was at least 75 percent molten since it impacted the cage wall and centers on a wire in a fraction of a second. This difference, if any, may be caused by acoustic streaming from the cold air injected by the sample insertion mechanism. If this is the case, then this effect would be intensified by going to higher acoustic power. An actual ground-based melt test will be conducted before the next flight to verify that this is not a problem.

Finally, it was recommended that a low-g test using the KC-135 be made on the all-up system. This was carried out at the end of July 1980, and the results summarized in Appendix XI indicate successful operation of the reconfigured acoustic levitator. During this test, sample capture occurred with g spikes approximately two orders of magnitude higher than nominally expected on SPAR.

By taking actions to reconfigure the apparatus by going to a cylindrical vibrator to allow higher acoustic power, to thoroughly test the apparatus using the KC-135, and to conduct laboratory tests for chamber resonance and acoustic vibrator fatigue it is felt that the most probable causes of failure on SPAR VI have been eliminated. By taking these actions it is felt that the probability of success for the next flight has been greatly enhanced.

APPENDIX I
ANALYSIS OF DAMPING

The axial amplitude decayed from 0.7 cm to 0.5 cm in five cycles.
The log decrement is

$$\delta = \ln (X_1/X_2) = 0.0057 \quad .$$

The equation of motion for a damped oscillator is

$$m\ddot{x} + \gamma\dot{x} + kx = 0 \quad .$$

The log decrement is related to the damping coefficient by

$$\delta = \frac{\gamma T}{2m} \quad .$$

For viscous damping, the drag is given by Stokes law,

$$F_D = 6 \pi \eta r v \quad ,$$

from which

$$\gamma = 6 \pi \eta r \quad .$$

The viscosity of air is given by kinetic theory as

$$\eta = \frac{1}{3} \frac{m\bar{v}}{\sqrt{2}\lambda} \quad ; \quad \bar{v} = \sqrt{\frac{8KT}{\pi m}} \quad .$$

At 373 K, $\eta = 2.18 \times 10^{-4}$ poise; therefore, at 1600 K,

$$\eta = 2.18 \times 10^{-4} \sqrt{\frac{1600}{373}} = 4.5 \times 10^{-4} \text{ poise}$$

$$\gamma = 6 \pi \eta r = 6 \pi (4.5 \times 10^{-4}) \quad (0.3)$$

$$= 2.54 \times 10^{-3} \frac{\text{dynes-s}}{\text{cm}} .$$

The calculated log decrement is

$$\delta = \frac{T\gamma}{2m} = \frac{(3.33 \text{ s}) (2.54 \times 10^{-3}) \text{ dyne-s}}{(2) (0.8) \text{ gm cm}} = 0.0053 .$$

This is very close to the observed value of 0.0057.

APPENDIX II

TEMPERATURE DEDUCED FROM SAMPLE POSITION

A shift of 0.2 cm was observed in the equilibrium position of the sample during the 35 s between sample deployment and loss from the potential well. The equilibrium position is located at $\lambda/4$ from the reflector. The change in λ is, therefore,

$$\Delta\lambda = 4\Delta\lambda = 0.8 \text{ cm} .$$

The velocity of sound is given by

$$C = \sqrt{\frac{\gamma kT}{m}} \quad 331 \text{ m/s at } 273 \text{ K}$$

$$C = 20.03 \sqrt{T} \text{ m/s} .$$

At $\nu = 15800 \text{ Hz}$,

$$\lambda = \frac{C}{\nu} = \frac{20.03}{15800} \sqrt{T} = 0.00128 \sqrt{T} \text{ m} = 0.128 \sqrt{T} \text{ cm} .$$

It was not possible to locate the sample accurately relative to the reflector in the flight film. However, it is assumed that temperature had recovered to approximately 1550°C when the sample was lost; the final value of λ was

$$\lambda_{\text{final}} = 0.128 \sqrt{1823} = 5.48 \text{ cm} .$$

If the original λ was smaller by 0.8 cm, the initial temperature must have been

$$T = \left(\frac{5.48 - 0.8}{0.128} \right)^2 = 1336 \text{ K} = 1063^\circ\text{C} .$$

The levitating force in a single-axis levitator goes as $T^{5/2}$. Therefore the decrease in force as the air temperature increases from 1336 K to 1823 K is

$$F = \left(\frac{1823}{1336}\right)^{-5/2} = 0.459 \ .$$

An initial restoring force of 2.9 dyne/cm at 1336 K would diminish to 1.33 dyne/cm at 1823 K. This is more than enough to explain the observed decrease to 1.6 dyne/cm after 17 s.

APPENDIX III

IMPULSIVE FORCE REQUIRED TO PRODUCE OBSERVED MOTION

Since the observed drift was perpendicular to the longitudinal axis, an impulsive angular acceleration could account for the observation.

The sample was observed to move from $x = 0.3$ to $x = 1.0$ in 2.3 s. The equation of motion is

$$\ddot{x} + \frac{K}{m} x = 0 \quad ; \quad t = 0 \quad , \quad x = x_1 \quad , \quad \dot{x} = v_0$$

$$x = A \sin \omega t + B \cos \omega t \quad ; \quad \omega = \sqrt{K/m}$$

$$\dot{x} = \omega A \cos \omega t - \omega B \sin \omega t$$

$$x(0) = B = x_1$$

$$\dot{x}(0) = \omega A = v_0 \quad ;$$

therefore,

$$A = v_0 \sqrt{m/K} = \frac{v_0 T}{2\pi}$$

The trajectory is

$$x(t) = \frac{v_0 T}{2\pi} \sin 2\pi \frac{t}{T} + x_1 \cos 2\pi \frac{t}{T}$$

$$x_1 = 0.3 \text{ cm} \quad , \quad T = 14.6 \text{ s}$$

$$x = 1 \text{ cm} \quad \text{at} \quad t = 2.3 \text{ s} \quad ;$$

therefore,

$$v_0 = 0.43 \text{ cm/s} \quad .$$

A kick of 0.43 cm/s corresponds to an instantaneous angular velocity of

$$\omega = \frac{v_o}{R} = \frac{0.43 \text{ cm}}{200 \text{ cm}} = 0.00215 \text{ rad/s} .$$

The corresponding velocity at the accelerometer (25 cm from the center of mass) is

$$v_a = (0.00215) (25 \text{ cm}) = 0.054 \text{ cm/s} .$$

This corresponds to an impulse of

$$I = \frac{0.054}{980} = 5.5 \times 10^{-5} \text{ g}\cdot\text{s} .$$

This is probably below the 10^{-4} g·s threshold of the instrument.

APPENDIX IV

ANALYSIS OF IMPULSE FROM BUBBLE RUPTURE

The following are calculations of the size of an air pocket in the oxide specimen which, if it ruptured, could have given the 0.8 gm specimen a 0.43 cm/s radial kick toward the cage.

The mass (m) of the gas ejecting at velocity (v) needed to give the specimen a kick is

$$mv = (0.8 \text{ gm}) (0.43 \text{ cm/s}) \quad .$$

Assume a bubble is formed at 30°C and that at approximately 1300°C the now pressurized bubble is released with the air ejected at the higher temperature sound speed v:

$$v \approx [3.3 \times 10^4 \text{ cm/s}] \left[\frac{1570 \text{ K}}{300 \text{ K}} \right] \approx 8.5 \times 10^4 \text{ cm/s} \quad .$$

Note that 1300°C is approximately the melting temperature of the oxide.

$$m = \frac{0.43 \times 0.8}{8.5 \times 10^4} = 4.04 \times 10^{-6} \text{ gram} \quad .$$

The density of air at STP is approximately $1.2 \times 10^{-3} \text{ gm/cm}^3$. This would correspond to a 1.9 mm diameter bubble at STP conditions.

In a 1300°C sample, such a bubble would have expanded to 3.4 mm diameter just before rupture. This would surely have been noticed in a 6 mm diameter sample.

APPENDIX V

EFFECT OF STEADY FORCE ON SAMPLE MOTION

Since the sample is observed to drift in a radial direction, it may be driven by centrifugal force resulting from a slow roll about the longitudinal axis. The equation of motion is

$$\ddot{x} + \frac{K}{m} x = \frac{F}{m} .$$

The solution is

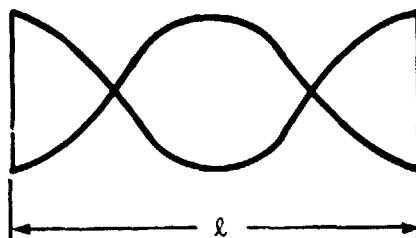
$$x = A_1 \cos \omega_0 t + A_2 \sin \omega_0 t + \frac{F}{m \omega_0^2} .$$

The effect of the constant F is simply to offset the oscillation by a fixed amount.

Since the acoustic levitator is located nearly on the longitudinal axis, F will actually be directly proportional to x . In this case it will simply diminish the restoring force K . This will simply increase the period of the oscillation and increase the amplitude.

APPENDIX VI
CONDITIONS FOR RESONANCE

For a chamber with fixed walls, the condition for resonance with an energy antinode in the center is



$$l = n\lambda \quad ; \quad n = 1, 2, 3, \dots$$

But

$$\lambda = \frac{C(T)}{\nu}$$

$$C(T) = \sqrt{\frac{\gamma RT}{M}} = 20.03 \sqrt{T} \quad ; \quad R = 8.31 \text{ J/mole K}$$

$$= 1.4$$

$$M = 28.9$$

$$\nu = 15.8 \times 10^3 \text{ Hz} \quad .$$

Resonance conditions at

$$l = \frac{n}{\nu} \sqrt{\frac{\gamma RT}{M}} = n \frac{2003}{15800} \sqrt{T} = 0.1268 n \sqrt{T} \text{ cm}$$

For 4.25 in. = 10.79 cm

n	T	
1	7241 K	(6968°C)
2	1810 K	(1537°C)
3	804 K	(531°C)

For 4.50 in. = 11.43 cm

n	T
1	8125 K (7852°C)
2	2031 K (1758°C)
3	903 K (630°C)

The observed drift was in the direction of the shortest wall (l = 4.25 in). It can be seen that the condition of resonance was approached as the chamber recovered to its original operating temperature.

APPENDIX VII

According to Gorkov,¹ the potential energy U of a body in an arbitrary standing wave field is

$$U \propto \left[\frac{P^2}{3\rho^2 c^2} \left(1 - \frac{c^2 \rho^2}{c_0^2 \rho_0^2} \right) - v^2 \left(\frac{\rho_0 - \rho}{2\rho_0 + \rho} \right) \right]$$

where c_0, ρ_0 and c, ρ are the density and sound speed of the body and medium, respectively. For a dense body in a gas

$$U \propto \left[\frac{P^2}{3\rho^2 c^2} - \frac{v^2}{2} \right]$$

where P and v are the pressure and velocity fluctuations.

For a single-axis suspension system, the forces along the axis (x direction) can be approximated by a plane standing wave (i.e., $P \sim v_0 \rho c \sin(kx)$ and $v \sim v_0 \cos(kx)$).

Hence the axial force $F_a = -\partial U / \partial x$

$$F_a \propto \left[\frac{2 \cdot k \cdot v_0^2}{3} \sin kx \cos kx + \frac{2 \cdot k \cdot v_0^2}{2} \cos kx \sin kx \right]$$

or the maximum

$$F_a \propto \frac{5 \cdot k \cdot v_0^2}{6} \propto \frac{5.3 v_0^2}{\lambda}$$

At a levitation node there is no pressure fluctuation; hence the radial force

1. L. P. Gorkov, Soviet Physics, Doklady, 6, 1962, p. 773.

$$F_r = - \frac{\partial u}{\partial r} \propto \frac{\partial \left(-\frac{v^2}{2} \right)}{\partial r}$$

or to an approximation

$$F_r \propto \frac{\Delta \left(\frac{v^2}{2} \right)}{\Delta r} \propto \frac{\left(\frac{v_o^2}{2} \cdot 0 \right)}{\left(0 - \frac{d}{2} \right)} \propto \frac{v_o^2}{d}$$

where d is the total transverse extent of the levitation well.

Forces at STP for an acoustic field of $\lambda \sim 2.5$ cm have been measured at MSFC using a 3.5 cm diameter driver and reflector. In this instance assume $d \sim 3.5$ cm, (i.e., the well dimension is roughly the size of the reflector, which is confirmed by holographs of the sound field).

Based on the preceding estimation, one would expect the ratio

$$\frac{F_r}{F_a} \approx \frac{\frac{v_o^2}{d}}{\frac{5.3 v_o^2}{\lambda}} \approx \frac{\lambda}{5.3 d} \approx \frac{1}{7} .$$

The experiments measured a ratio

$$\frac{F_r}{F_a} \approx \frac{1}{10} .$$

Intersonics, Inc., has studied the acoustic capture using a 2.5 cm reflector at 1250° to 1550°C for a field of $\lambda \sim 5$ cm. For this case, since the reflector size $\ll \lambda$, assume that $d \sim \lambda$, since one would expect an interference well between the initial and reflected wave to extend a transverse distance λ in front of the reflector.

$$\frac{F_r}{F_a} \approx \frac{\lambda}{5.3 (d = \lambda)} \approx \frac{1}{5} .$$

Intersonics measurements indicate

$$\frac{F_r}{F_a} \sim \frac{1}{8}$$

The theoretical calculations and data are in general agreement. For convenience it is reasonable to assume that

$$\frac{F_r}{F_a} \sim \frac{1}{10}$$

for most cases of interest.

APPENDIX VIII

In a stable capture in a stationary acoustic field, a dense body will oscillate about the central node with an angular frequency W . In a manner analogous to a simple harmonic oscillator we can define a spring constant κ where $\kappa = W^2 M$, M being the body mass. The maximum restoring force would be approximated by $\kappa \ell$, where for the case of a plane stationary wave $\ell = \lambda/8$. The acoustic restoring force is proportional to the body volume V ; therefore, to obtain a parameter that is dependent only upon acoustic parameters, we will define a normalized maximum restoring force $= \kappa \ell / v$. (A more rigorous treatment of body oscillations in an acoustic field is provided by King in his classic paper on acoustic forces.¹) A plane stationary wave is a good approximation for the field in a 3-axis system and along the axis in a 1-axis system. However, for the radial forces in a 1-axis device and for a small reflector, assume that the well extends a transverse distance $\sim \lambda$ and that the point of maximum force is halfway between the center and edge (i.e., $\ell \sim \lambda/4$).

The capability of the well to maintain capture against a constant acceleration a is $M a = \kappa \ell$

$$a = \frac{\kappa \ell}{M} = \frac{\kappa \ell}{\rho_0 V}$$

where ρ_0 is the body density.

If the body is given an impulse ($g \Delta T$) resulting in a velocity $v = g \Delta T$, the capability of the well to maintain capture is determined by

$$\frac{1}{2} M v^2 = \frac{1}{2} M (g \Delta T)^2 \leq \frac{1}{2} \kappa x^2$$

or

$$g \Delta T \leq \left(\frac{\kappa x^2}{\rho_0 V} \right)^{1/2}$$

1. King, Proc. Royal Soc., A147, 1934.

It is assumed that the height of the potential well is roughly that estimated from the point of maximum force (i.e., $x = \ell$, $\sim \lambda/8$ for a 3-axis system and $\sim \lambda/4$ for the radial component of a 1-axis system).

The normalized maximum restoring force, the maximum constant acceleration, and the maximum impulse are given in Table I for a variety of experiments and measurements of the single-axis acoustic system at high temperature. Also included for comparison are the same parameters for the SPAR VI flight of the 3-axis system.

TABLE 1. QUALITY OF SINGLE-AXIS ACOUSTIC CAPTURE VERSUS WELL STRENGTH

Example	Capture Probability	Normalized Maximum Radial Force ³ (dyne/cm ²)	Maximum Constant Acceleration (a) Needed to Overcome Well (cm/s ²)	Maximum Impulse Needed to Overcome Well (cm/s)	Furnace Temperature (°C)	Body Density (gm/cm ³)	Comments
SPAR VI (E)	Lost sample	0.8	0.2	0.45	1500	0.4	Radial motion very difficult to interpret.
KC 135 Sept 1977 Sound Level I 139 dB (G)	No apparent capture	1.2	4	2	1200	0.3	Furnace temperature rapidly varying.
KC 135 Sept 1977 Sound Level II 143 dB (G)	Occasional capture	3.0	10	3.2	1200	0.3	Furnace temperature rapidly varying.
Laboratory pend. measurements 6 A to Driver (G')	No capture	3.5	11.5	3.4	1500	0.3	Thermal convection masks any capture.
Laboratory pend. measurements 8 A to Driver (G)	Capture	6	20	4.5	1500	0.3	Capture observed over thermal convection.
KC-135 Sept 1977 Sound Level III 147 dB (G)	Some captures	7.5	25	5	1200	0.3	Cylindrical body used, often spinning, furnace temperature varying.
KC 135 June 1978 Sound Level 154 dB (M)	Solid capture	15	45	6.7	1550	0.3	Capture generally very evident.
SPAR VI Axis System (v)	Solid capture	3	3	3	30	1	Initial drop perturbation very small

(M) - Period directly measured.

(E) - Axial period measured, radial assumed 1/10 axial.

(G) - Period directly measured for sound level II, radial forces for sound levels I and III assumed proportional to acoustic intensity.

(G') - Directly measured for 8A to driver, radial forces assumed proportional to input power (i.e., current²) to transducer.

APPENDIX IX

SUMMARY REPORT OF FATIGUE TESTS OF CYLINDRICAL VIBRATORS

Fatigue testing of 10 cylindrical vibrators used in the St. Clair sound source have been completed. These tests consisted of driving the vibrator using a flight-configured magnet with the vibrator mounted in the same configuration as the flight unit. The end deflection of each vibrator was periodically measured directly by means of examination with a calibrated microscope. Since fatigue failures are dependent on the number of cycles, it was decided to test at least 10^8 cycles which represent at least an hour of continuous operation. The number of cycles thus was sufficient to ascertain the asymptotic limit of stress for an infinite number of cycles.

The stress level in most cases was initially low and was increased when it was determined that no failures were occurring at that stress level. Systematically end deflections were gradually increased beginning at 1 mil peak-to-peak. Figure IX-1 summarizes the number of cycles at varying strain levels.

No failures have been observed at levels less than 6 mils peak-to-peak. One apparent failure, which resulted in a slight degradation of output amplitude, occurred after 10^7 cycles at an amplitude of 6.3 mils peak-to-peak. This event occurred in a vibrator which had a relatively short history of testing at lower levels, but occurred when the vibrator temperature was in excess of 120°C .

It has been concluded that vibrator amplitudes of up to 4 mils peak-to-peak can be maintained indefinitely without fatigue failures. This result is in agreement with the limits of 6 mils peak-to-peak suggested as an upper limit in the letter to R. Chassay from J. B. Sterrett dated July 22, 1980, concerning a MSFC stress analysis of the vibrator for the acoustic levitator. It is planned at this time that the amplitude to be used on the SPAR VIII flight of the acoustic levitator will not exceed 4 mils peak-to-peak.

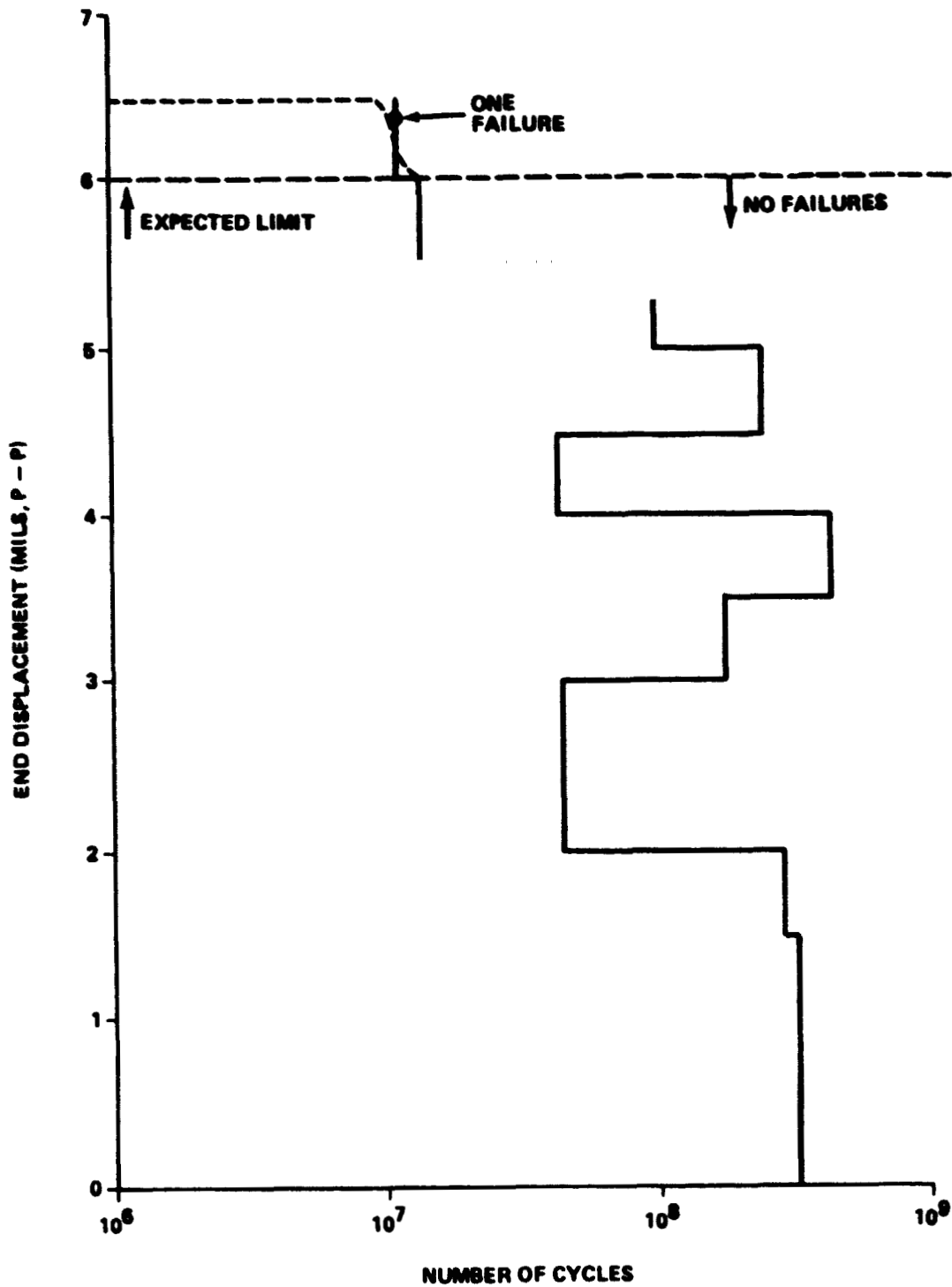


Figure IX-1. Fatigue tests of cylindrical vibrators.

APPENDIX X

SUMMARY REPORT OF GROUND-BASED TESTS ON ACOUSTIC LEVITATOR

Cold injection tests were performed using the spring pendulum and inserting a cold reflector/injector assembly into the acoustic levitator furnace at temperatures up to 1600°C. No perturbations or abnormalities in positioning were observed even for times up to 5 minutes of continuous positioning.

Acoustic cavity resonance search: Efforts to observe acoustic resonance in the furnace cavity were made over a range from 900 - 1600°C, again using the spring pendulum. No deflections from the equilibrium position were observed and no evidence of any resonances or other position perturbing effects were apparent.

During all of the spring pendulum tests the equilibrium position of the specimen with no sound in the cavity was adjusted to ± 5 mm in the axial direction and up to 11 mm in various radial directions. This insured that any tendency for an instability to occur would be enhanced rather than suppressed by the restoring forces of the spring pendulum. In addition to the equilibrium point displacement, with the sound turned off one could observe thermal convection random deflections in all directions of approximately ± 5 mm. During positioning with the sound on and the specimen in place the specimen remained steady over wide temperature ranges and when intentionally perturbed would perform simple harmonic oscillations from which restoring forces were calculated. For instance, at 1575°C temperature 93 dynes/cm restoring force was obtained in the axial direction and 7.5 dynes/cm radially at a sound pressure level of 159 db.

Higher density specimen tests: Tests similar to those referred to in A and B above were performed with a denser test specimen in order to verify that specimen density could not adversely affect positioning reliability. Initially a test specimen weighing 50 mg was used, but this was replaced by a specimen of 620 mg. The denser specimen had an effective density of 4.3 gm/cm^3 . In all tests the denser specimen appeared to have a greater stability than the less dense one. This is not surprising, in as much as the small residual fluctuations are produced by random thermal air currents acting on the pendulum string and wire. However, it should be noted that residual accelerations of the levitator frame of reference (as could conceivably have occurred in the SPAR VI Payload) would produce larger perturbations in the specimen position proportionally as the density of the specimen was increased. We estimate that for the flight specimen density and a sound level of 159 db that it would require residual g forces in excess of about 10,000 micro g's to dislodge the specimen from the energy well.

APPENDIX XI

KC-135 TESTING OF THE ACOUSTIC LEVITATOR FURNACE SUBASSEMBLY

A number of parabolas were flown and, although about 8 parabolas show periods of very low residual g forces, successful injections were obtained and stable positioning achieved for a larger subset of parabolas. In those cases where a 3-axis accelerometer indicated excessive g forces, uncontrolled specimen motion occurred. This was true in general for accelerations in excess of 3000 micro g's when sound pressure levels were below 157 db (Fig. IX-1). Repeated cycling of the flight hardware during this KC sequence of tests indicated a high level of reliability of this equipment.

Parabola Number	Residual G Levels (m g)	Specimen Capture Code (1)	Performance Satisfactory	
Day 1	1	10	YES	
	2	3		
	3	4		
	4	7		
	5	9	YES	
	6	8	YES	
	7	9	YES	
	8	7		
	9	1,8		
	10	10	YES	
	11	8	YES	
Day 2	1	0		
	2	0		
	3	0		
	4	6	YES	
	5	1		
	6	7	YES	
	7	8	YES	
	8	4		
	9	8	YES	
Day 3	6	7		
	7	(10) 1,5	(NO) YES	
	8	8	YES	
	9	9	YES	
	10	10		
	11	1	9	YES
	12	8	4	
	13	6	2	
	14	3	9	YES
	15	6	8	YES
	16	8	6	
	17	10	4	
	18	6	7	
	19	2	3	YES
	20	5	9	YES
	21	8	7	
	22	10	4	
	23	4	5	
	24	6	3	
	25	2	10	YES
	26	8	4	
	27	4	8	YES
	28	6	6	
	29	6	8	YES
	30	8	9	YES

(1) 10 is perfect, 0 is no positioning at all, 6 or better indicates good injection and capture, 1 through 5 correspond to varying levels of positioning.

Figure XI-1 Data summary of KC-135 low g test of acoustic levitation.

APPROVAL

POSTFLIGHT ANALYSIS OF THE SINGLE-AXIS ACOUSTIC SYSTEM ON SPAR VI AND RECOMMENDATIONS FOR FUTURE FLIGHTS

By R. J. Naumann, W. A. Oran, Roy R. Whymark, and Charles Rey

The information in this report has been reviewed for technical content. Review of any information concerning Department of Defense or nuclear energy activities or programs has been made by the MSFC Security Classification Officer. This report, in its entirety, has been determined to be unclassified.



CHARLES A. LUNDQUIST

Director, Space Sciences Laboratory